metals

MDPI

Article

Feasibility of a Two-Stage Forming Process of 316L Austenitic Stainless Steels with Rapid Electrically Assisted Annealing

Viet Tien Luu [1], Thi Anh Nguyet Nguyen [1], Sung-Tae Hong [1,*], Hye-Jin Jeong [2] and Heung Nam Han [2]

1 School of Mechanical Engineering, University of Ulsan, Ulsan 44610, Korea; tienvietluu@gmail.com (V.T.L.); sweetmoona2@gmail.com (T.A.N.N.)

2 Department of Materials Science & Engineering and Center for Iron & Steel Research, RIAM, Seoul National University, Seoul 08826, Korea; hj8262@snu.ac.kr (H.-J.J.); hnhan@snu.ac.kr (H.N.H.)

* Correspondence: sthong@ulsan.ac.kr; Tel.: +82-52-259-2129

Received: 27 September 2018; Accepted: 8 October 2018; Published: 11 October 2018

check for updates

Abstract: The post-annealing mechanical behavior of 316L austenitic stainless steel (SUS316L) after electrically assisted (EA) annealing with a single pulse of electric current is experimentally investigated to evaluate the feasibility of a two-stage forming process of the selected SUS316L with rapid EA annealing. A tensile specimen is deformed to a specific prestrain and then annealed by applying a single pulse of electric current with a short duration less than 1 s. Finally, the specimen is reloaded until fracture. The stress-strain curve during reloading shows that the flow stress of the SUS316L significantly decreases, which indicates the occurrence of EA annealing. The electric current also increases the maximum achievable elongation of the SUS316L during reloading. The stress-strain curve during reloading and the microstructural observation suggest that the effects of EA annealing on the post-annealing mechanical behavior and microstructure strongly depend on both the applied electric current density (electric current per unit cross-sectional area) and the given prestrain. The results of the present study suggest that the EA annealing technique could be effectively used to improve the formability of SUS316L when manufacturing complex parts.

Keywords: electrically assisted annealing; electric current; prestrain; stainless steels

1. Introduction

Formability is an important issue for all metallic materials in forming processes, even for austenitic stainless steels (ASSs). ASSs are known to have good formability, excellent corrosion resistance, and good weldability [1–3]. However, in some industrial applications, the good formability of ASSs may still not be satisfactory [4,5]. For example, in deep drawing of consumer electric components using ASSs, the forming process is frequently composed of two (or multiple) forming stages with heat treatment between the forming stages, due to the formability of the ASSs.

Furnace annealing between forming stages is a commercially well-established heat treatment process to control the formability of an ASS in a two- or multiple-stage forming process. A deformed part is heat-treated in a certain temperature range (800–1100 °C) for a specified duration (usually from 30 to 45 min) [4,5] before the next forming stage. While furnace annealing can effectively restore the formability of the product by annihilating strain hardening from the previous forming stage, furnace annealing frequently becomes quite time-consuming and expensive. Thus, a cost-effective and preferably rapid alternative technique to control the formability of ASS is still desirable.

Electrically assisted manufacturing (EAM) is a promising metal forming technique, in which the mechanical property of a metal is controlled by simply applying electricity to the metal during deformation (referred to as electroplasticity) [6,7]. In the investigation of the effect of electric current on the mechanical behavior of metal alloys, several researchers repeatedly applied electric current with a short duration (pulsed electric current) to a metal during deformation. Roth et al. [8] applied a pulsed electric current to aluminum 5754 alloy during tension to achieve maximum elongation close to 400% of the gage length. Salandro et al. [9] applied a pulsed electric current to aluminum 5052 and 5083 alloys during tension. According to Salandro et al. [9], the effectiveness of the electric current on the tensile behavior of selected aluminum alloys depends on both the alloy and the heat treatment. Kim et al. [10] and Roh et al. [11] reported that the formability of aluminum alloys during tension with a pulsed electric current is increased due to electric current induced (or electrically assisted: EA) annealing. It has also been reported that the microstructure of metals can be significantly affected by electric current. Conrad et al. [12] reported that the plasticity and phase transformation of various metals and ceramics were affected by an electric current. Xu et al. [13] reported that recrystallization and grain growth of cold-rolled α-Ti were accelerated by an electric current. More recently, Park et al. [14] reported that the annealing temperature and time for recrystallization of interstitial free (IF) steel and AZ31 magnesium alloy were significantly reduced by electropulsing treatment (EPT) compared to conventional heat treatment with a furnace. It is important to note, however, that for specific metal alloys and experimental conditions, applying an electric current during deformation may induce adverse effects on the formability [15,16]. Magargee et al. [15] observed that the formability of commercially pure titanium was not significantly changed when an electric current was applied during tensile deformation, even though the flow stress substantially decreased. Jeong et al. [16] studied the effect of electric current on the tensile behavior of transformation-induced plasticity (TRIP)-aided steel and reported that the elongation of TRIP-aided steel significantly decreased by applying a pulsed electric current during tensile deformation. They suggested that the effect of electric current on the mechanical behavior can be strongly affected by designing the pulsing pattern of the electric current in accordance with the material's characteristics.

While applying a pulsed electric current to a metal alloy during deformation generally enhances the formability of the metal alloy, it may not be practical to design a commercial metal forming process with a pulsed electric current. The cycle time of the process may be significantly increased and/or the structure of forming machines may become quite complex. Several recent studies on EAM or electroplasticity have reported that the mechanical properties of a metal can be altered by applying a single pulse of electric current of short duration. Kim et al. [17] reported that the springback in U-bending of advanced high strength steel sheets can be reduced or even eliminated by applying a single pulse of electric current prior to removal of the forming load. Thien et al. [18] applied a single pulse of electric current to a complex phase ultra-high strength steel at a specific prestrain and reported that the flow stress significantly decreased and the formability increased during reloading. These previous studies suggest that electrically assisted two- (or multiple-) stage metal forming processes for certain metal alloys may be effectively designed with a single pulse of electric current.

However, studies on the mechanical behavior of metal alloys (including ASSs) under a single pulse of electric current between plastic deformations are still quite limited. In the present study, the effect of a single pulse of electric current on the mechanical behavior and microstructure of a commercially available 316L austenite stainless steel (SUS316L) is reported. Specifically, the goal of the present study is to evaluate the feasibility of a two-stage forming process of the selected SUS316L with rapid EA annealing.

2. Experimental Set-Up

Commercially available 1 mm thick grade SUS316L sheets (Fe-17.06Cr-9.81Ni-1.17Mn-1.97Mo-0.59Si-0.028C in wt.%) were used for the experiment. Typical tensile specimens according to ASTM-E08 with a gage width of 12.5 mm and a gage length of 50 mm were fabricated by laser cutting along the rolling direction of the sheet.

In the present study, electrically assisted (EA) two-stage forming of the selected SUS316L was simply implemented by quasi-static tensile tests with a single pulse of electric current, as schematically described in Figure 1. The quasi-static tensile test was conducted using a universal testing machine. The baseline tensile test was first conducted by simply deforming a specimen by tension until fracture. For the quasi-static tensile test with EA annealing, a specimen was first deformed to a specified prestrain by uniaxial tension with a constant displacement rate of 2.5 mm/min. A single pulse of electric current with a short duration was then applied to the prestrained specimen to induce EA annealing, according to the electric current parameters. Next, the specimen was cooled to room temperature in air and unloaded. Finally, the specimen was reloaded until fracture by uniaxial tension with a constant displacement rate of 2.5 mm/min.

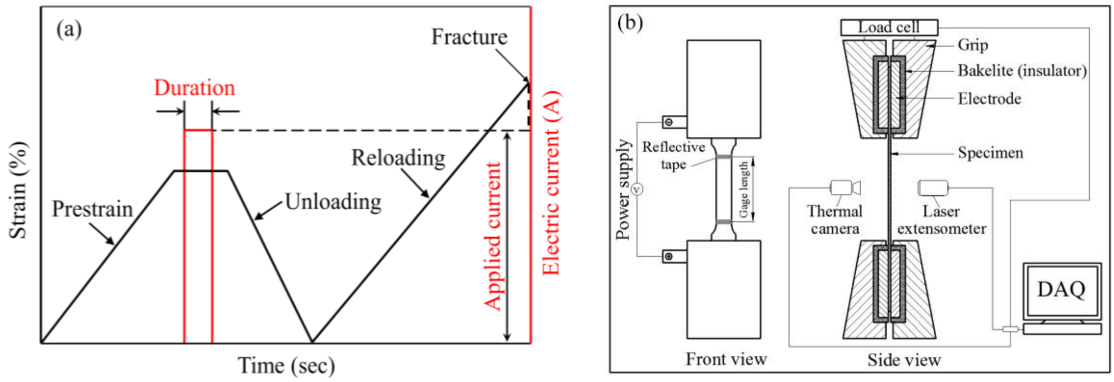

Figure 1. Schematics of (**a**) electrically assisted (EA) annealing with a single pulse of electric current and (**b**) the experimental set-up.

For EA annealing, the electric current was generated by a programmable Vadal SP-1000U power supply (Hyosung, Seoul, Korea). By inserting a set of bakelite insulators between the specimen and grips, the tensile test machine was insulated from the electric current (Figure 1b). The force history during the experiment was measured as a function of time by a load cell using a PC-based data acquisition system (Figure 1b). The displacement history was also measured using a laser extensometer (LX500, MTS, Eden Prairie, MN, USA) by attaching retro-reflective tape to the specimen. Finally, an infrared thermal imaging camera (T621, FLIR, Taby, Sweden) was employed to monitor the temperature change of the specimen throughout the experiment. It should be noted that one side of the specimen was sprayed with black thermal paint to stabilize the emissivity and thus improve the accuracy of the temperature measurement. The emissivity was calibrated by a k-type thermocouple through separate calibration tests.

For the parameter study, two different prestrain levels (20% and 60%) were combined with three different true electric current densities (95, 100, and 105 A/mm^2) and a constant electric current duration of 0.75 s. It should also be noted that the selected prestrains in the present study correspond to 20% and 60% of uniform elongation from the baseline tensile test (without prestrain and electric current), respectively, as indicated in Figure 2. The true electric current density was calculated based on the actual cross-sectional area of the specimen at the given prestrain, as the term "true" indicates. For each parameter set, at least three specimens were tested to verify repeatability of the results.

To analyze the effect of electric current on the microstructure of a prestrained specimen, the EA annealed specimen was removed from the test without reloading to fracture and was prepared for microstructural analysis. The microstructure of the specimen was characterized by an electron probe microanalyzer (EPMA, JXA-8530F, JEOL Ltd., Tokyo, Japan) and a field emission gun scanning electron microscope (FE-SEM, SU70, Hitachi, Tokyo, Japan) equipped with an electron backscatter diffraction system (EBSD, EDAX/TSL, Hikari, Hayward, CA, USA). To evaluate the change of dislocation density by EA annealing, the full width at half maximum (FWHM) of the diffraction peak was measured with an X-ray diffractometer (D8-Advanced, BRUKER MILLER Co., Boston, MA, USA) using a Cu radiation source operating at 50 kV at room temperature. Diffraction patterns were recorded in the scan range of 40–85° with a scan speed of 1°/min. Specimens for microstructural observation were prepared by mechanical grinding followed by electropolishing with an 80 mL perchloric acid, 90 mL distilled water, 100 mL butanol, and 730 mL ethanol solution at 20 V. For EBSD analysis, the accelerating voltage and scan step size were 15 kV and 0.5 µm, respectively. The critical misorientation angle was set to 15° for grain identification.

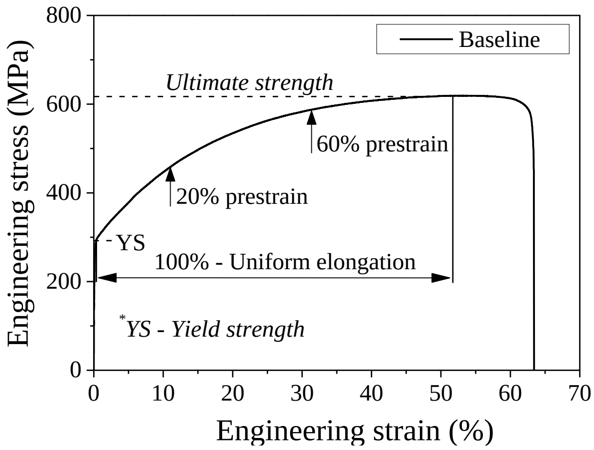

Figure 2. A stress–strain curve of a baseline specimen.

3. Results

During EA annealing, the temperature of the specimen rapidly reached the maximum temperature using resistance heating followed by cooling, as representative temperature histories of the 60% prestrained specimens shown in Figure 3a. It should be noted that the temperature was measured at the center of the specimen, which gave the highest temperature from application of the electric current. Naturally, the peak temperature increased as the current density was increased as shown in Figure 3b. Additionally, there was no significant effect of two different prestrains on the peak temperature.

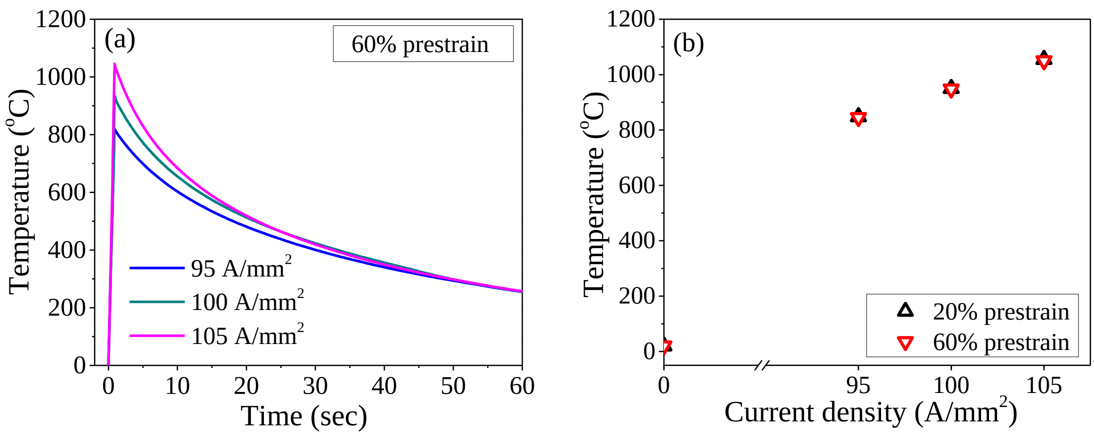

Figure 3. (**a**) Temperature histories of 60% prestrained specimens and (**b**) the peak temperatures as functions of current density during EA annealing for different prestrains.

From the load-displacement history during reloading, engineering stress-strain curves during reloading were constructed based on the gage length and cross-sectional area at each prestrain, as shown in Figure 4. As expected, the yield strengths during reloading (the post-annealing yield strengths) generally showed higher values than the baseline yield strength without prestrain due to strain hardening for both prestrains. For the same reason, the elongations at fracture during reloading (the post-annealing elongation) for both prestrains generally showed lower values than the baseline elongation at fracture without prestrain. As the current density was increased, the engineering stress-strain curves during reloading clearly showed that the flow stress of the SUS316L gradually decreased, which indicates the occurrence of EA annealing [10]. The post-annealing elongation also clearly increased with increasing current density.

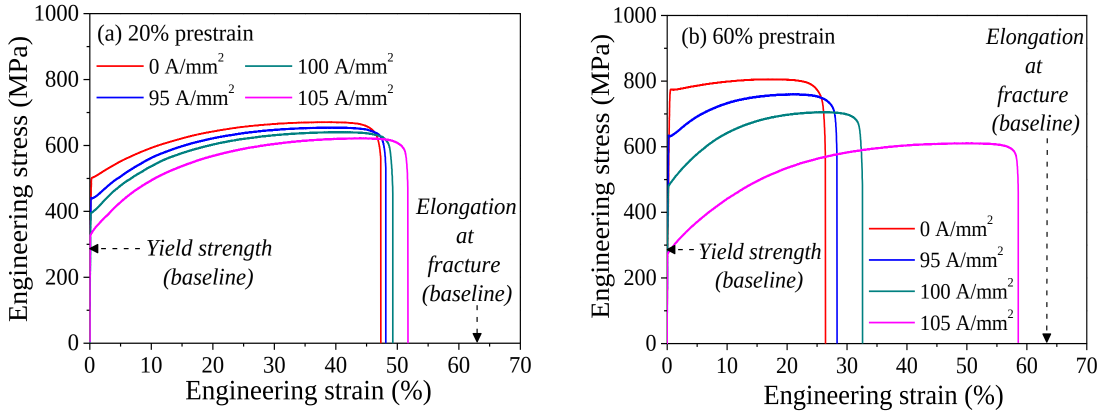

Figure 4. Engineering stress-strain curves after EA annealing with (**a**) 20% prestrain and (**b**) 60% prestrain; the engineering stress-strain curves during reloading was constructed based on the gage length and the cross-sectional area at each prestrain.

The post-annealing yield strength and post-annealing elongation can be plotted as functions of current density (Figure 5a,b, respectively). The results in Figure 5a,b suggest that the effect of EA annealing on the mechanical behavior during reloading is significantly different depending on the magnitude of the prestrain, even with the same true current density and nearly identical peak temperatures. As shown in Figure 5a,b, with the higher prestrain, the effect of EA annealing becomes more pronounced, i.e., the post-annealing yield strength and post-annealing elongation change more rapidly with the higher prestrain, as the current density increases with the constant duration of electric current. The effectiveness of EA annealing on the formability of the SUS316L can be further evaluated by comparing the total achievable displacement or total achievable elongation based on the original gage length of the baseline specimen. The total achievable displacement and total achievable elongation can be simply calculated as:

Total achievable displacement = displacement by prestrain + displacement during reloading

Total achievable elongation = total achievable displacement/the gage length of the baseline specimen

The total achievable elongation as a function of current density, clearly seen in Figure 6a,b, confirms that EA annealing at the higher prestrain is beneficial to improve formability of the given metal alloy. Especially at the highest current density of 105 A/mm^2, the total achievable elongation with the 60% prestrain was approximately 1.5 times higher than that with the 20% prestrain (Figure 6a,b). It is to be noted that the total achievable elongation with the 20% prestrain and current density of 95 A/mm^2 still surpassed that of the baseline tensile test.

For evaluation of the effect of EA annealing on hardening behavior during reloading, the engineering stress-strain curves in Figure 4 were converted to true stress-strain curves up to the engineering strain of uniform elongation, as shown in Figure 7a,b. As expected, strain hardening parameters with the higher prestrain showed lower values in comparison to those with the lower prestrain. However, the strain hardening exponent (Figure 7c) and strength coefficient (Figure 7d) as functions of current density showed that with the higher prestrain, both strain hardening parameters increased more rapidly as the current density was increased. At the current density of 105 A/mm^2, the strain hardening parameters during reloading with the 60% prestrain became nearly identical to those of the baseline curve without prestrain. This finding suggests that the strain hardening by the given prestrain was completely annihilated by the electric current with a duration of 0.75 s, which confirms the benefit of EA annealing as a rapid annealing process for cost-effective two-stage forming. However, it should be noted that with the 20% prestrain, the strain hardening parameters during reloading were not close to those of the baseline curve without prestrain, even at the current density of 105 A/mm^2, which was the highest current density selected in the present study. Therefore, in the design of two-stage forming with EA annealing, the amount of deformation in the first forming stage needs to be carefully decided to optimize the effect of EA annealing in the process.

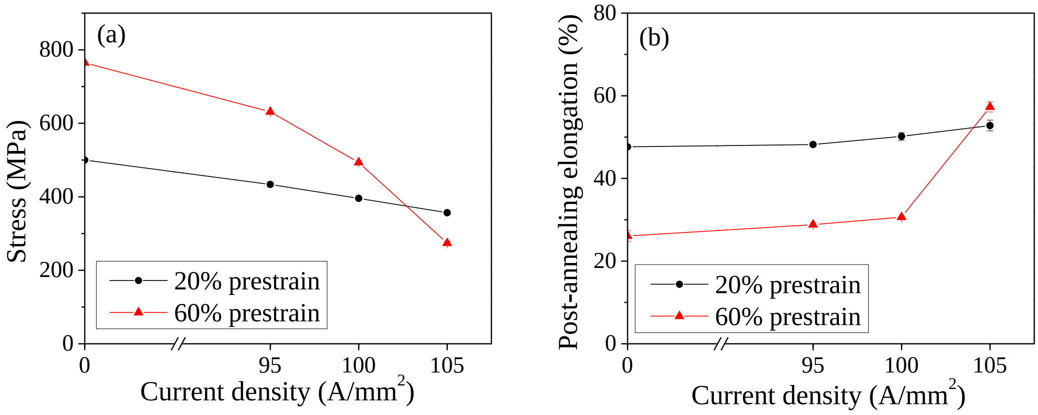

Figure 5. (**a**) Post-annealing yield strength and (**b**) post-annealing elongation of prestrained specimens after EA annealing.

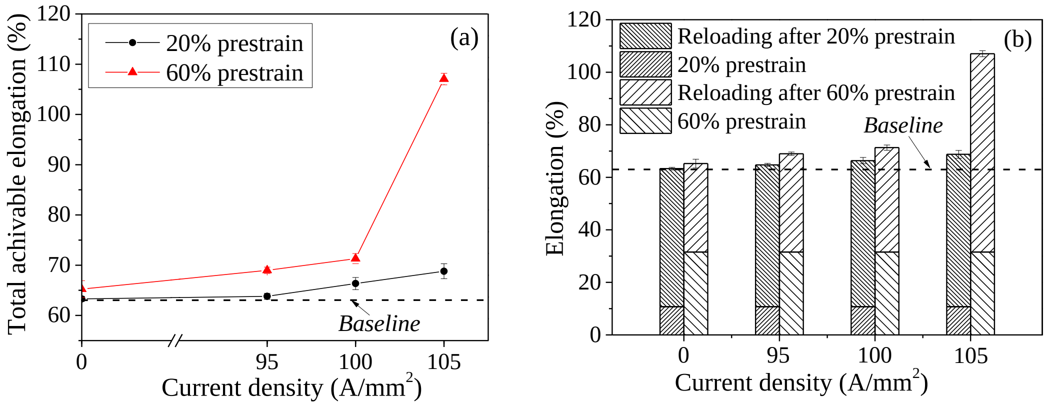

Figure 6. (**a**) Total achievable elongation as a function of current density and (**b**) the effect of prestrain and the current density on the total achievable elongation; the total achievable elongation was calculated based on the original gage length of the baseline specimen.

As presented above, the mechanical behavior of the SUS316L during reloading after a short duration of electric current strongly suggests the occurrence of EA annealing. To confirm this occurrence of EA annealing, FWHM analysis of the diffraction peak profile can be effectively used [19,20]. For crystalline materials, the diffraction peak profile is typically broadened when the crystal lattice is distorted by lattice defects, especially by dislocations [21,22]. As shown in Figure 8a,b, the FWHM values decreased with increasing current density for both prestrains selected in the present study. The results in Figure 8a,b clearly confirm the reduction of dislocation density (annihilation of dislocations) in the prestrained specimen by the applied electric current, which is EA annealing. It should be noted that for the 60% prestrain, the FWHM values show that the specimen was fully annealed to the baseline status without prestrain when the electric current density of 105 A/mm^2 was applied. Therefore, it is speculated that recrystallization occurred under this condition. In contrast, for all of the 20% prestrained specimens, full annealing was not achieved, even though the peak temperatures were nearly the same, as shown in Figure 3b. The results of the FWHM analysis are in good agreement with the observed mechanical behavior during reloading after EA annealing in Figures 4–6.

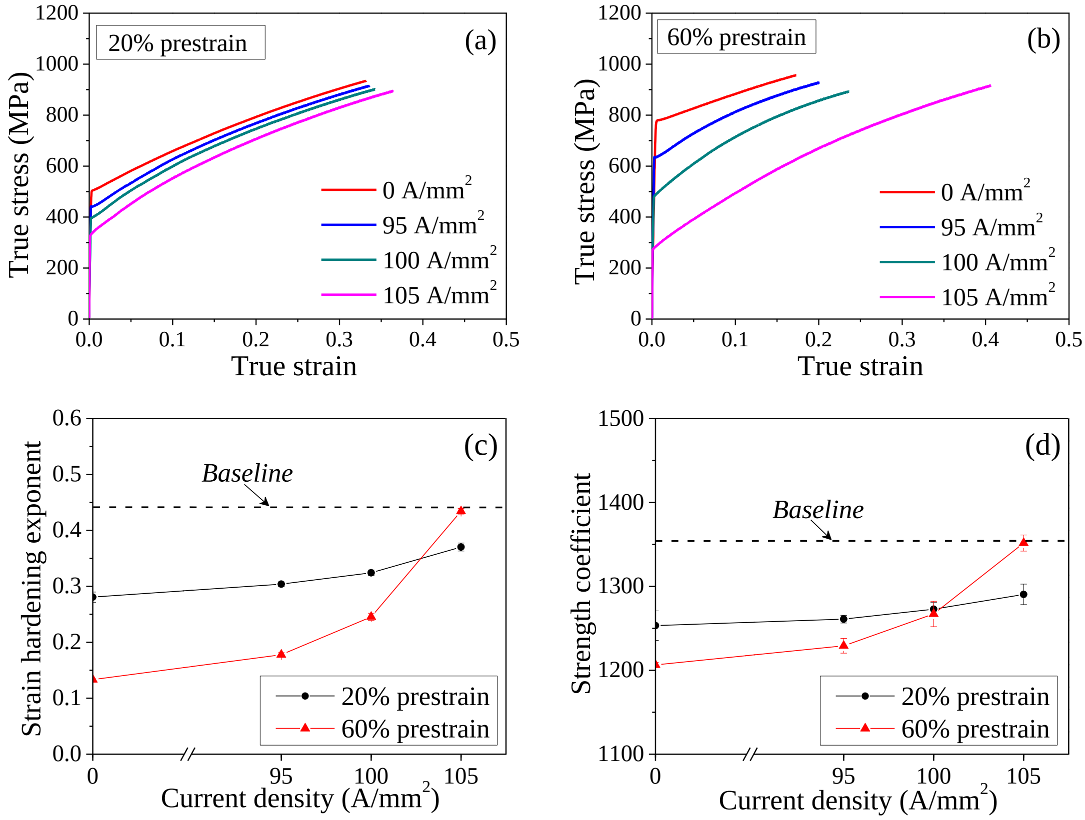

Figure 7. True stress-strain curves after EA annealing with (**a**) 20% prestrain and (**b**) 60% prestrain; (**c**) strain hardening exponent and (**d**) strength coefficient of prestrained specimens after EA annealing.

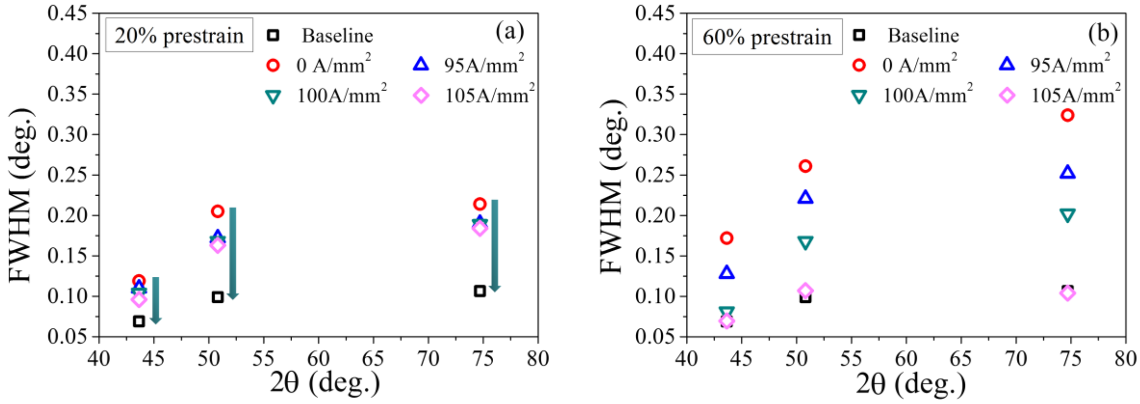

Figure 8. Full width at half maximum (FWHM) profiles of specimens with (**a**) 20% prestrain and (**b**) 60% prestrain.

Figure 9 shows the EBSD inverse pole figures (IPF) with respect to the normal direction (ND) and kernel average misorientation (KAM) maps for each specimen. For KAM maps, the higher degree of misorientation is denoted by a brighter color. The color of the KAM maps is proportional to the amount of dislocation or the accumulated strain energy present in the specimen, as indicated in the color scale bar. The KAM maps display effects, which can be interpreted as dislocations. For EA annealing with 105 A/mm^2, the average grain size of the 60% prestrained specimen was significantly reduced from 17.0 ± 5.9 to 12.1 ± 4.3 μm. The average KAM value of the 60% prestrained specimen was also significantly reduced from 1.10 to 0.33 under the condition of 105 A/mm^2. This result clearly indicates that recrystallization occurred in the 60% prestrained specimen after EA annealing with the current density of 105 A/mm^2. This result coincides with the FWHM value of the 60% prestrained specimen under the electric current density of 105 A/mm^2, as shown in Figure 8b. This result can be explained as the dislocation density induced by the 60% prestrain was high enough to provide the driving force for recrystallization [23] during EA annealing with 105 A/mm^2 for the duration of 0.75 s. This phenomenon might be related to the acceleration of recrystallization kinetics due to the electric current [14]. No significant changes in the grain size were observed for the other combinations of prestrain and electric current density considered in the present study.

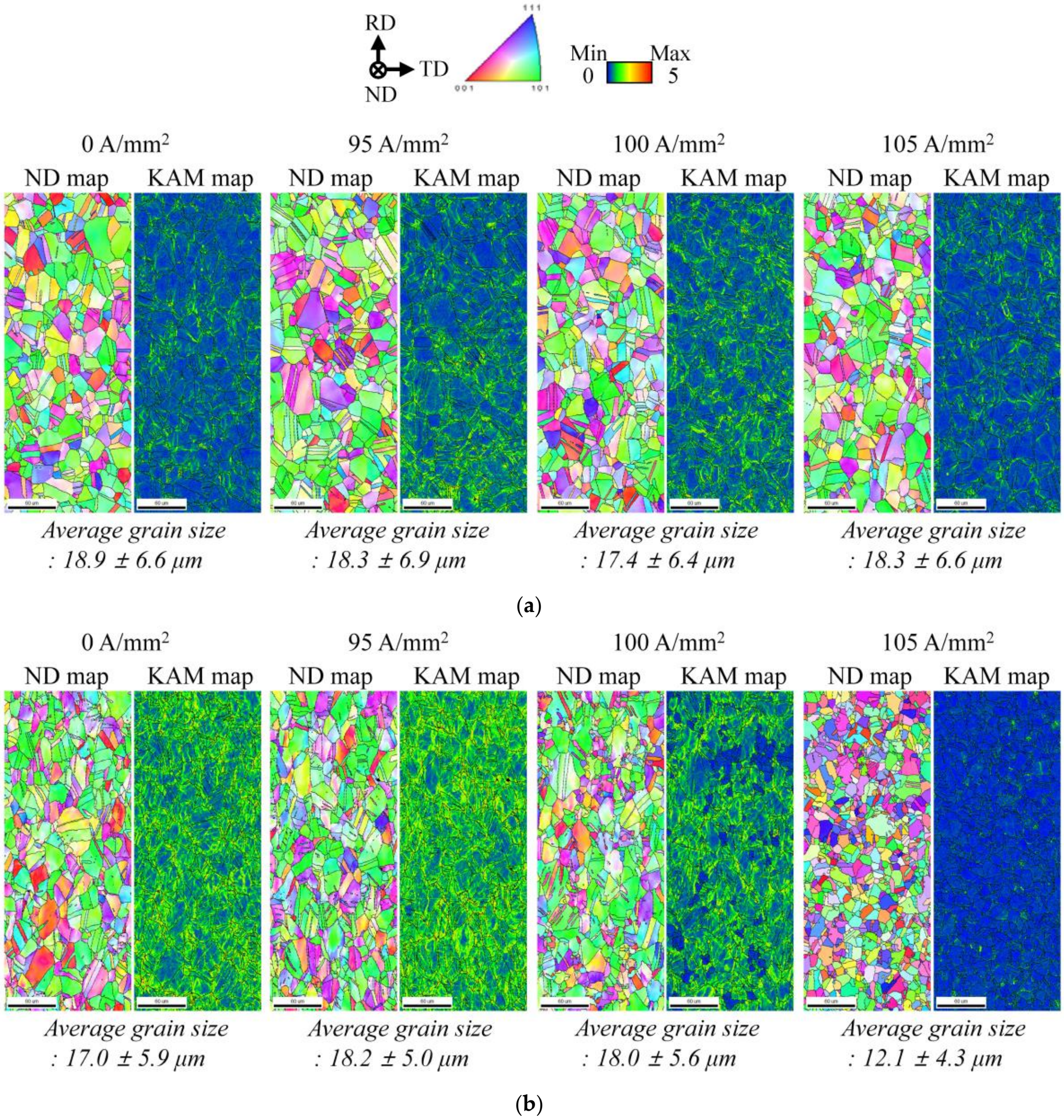

Figure 9. Electron backscatter diffraction (EBSD) inverse pole figures for normal direction (ND) and kernel average misorientation (KAM) maps of specimens with (**a**) 20% prestrain and (**b**) 60% prestrain for various electric current densities.

4. Conclusions

In the present study, the effects of a single pulse of electric current on the mechanical behavior and microstructure of a commercially available SUS316L were investigated to evaluate the feasibility of a two-stage forming process with rapid EA annealing in less than 1 s. The mechanical behavior of the prestrained specimen after applying a single pulse of electric current to the specimen suggests the occurrence of EA annealing. The results of microstructural analysis show the annihilation of dislocations by the electric current, confirming the occurrence of EA annealing. The experimental results show that the effectiveness of EA annealing strongly depends not only on the electric current parameters, but also the magnitude of the prestrain. Depending on the electric current parameters and the magnitude of the prestrain, full annealing with recrystallization was even possible to significantly increase the total maximum achievable elongation of the specimen. The results of the present study suggest that a two-stage forming process of SUS316L can be simplified and expedited by properly implementing rapid EA annealing in the process. As a final remark, in the present feasibility study, the duration of electric current was fixed for simplicity. However, for optimization of a practical dual-stage forming process with rapid EA annealing, a further study with expanded electric current parameter combinations with different electric current durations may be necessary.

Author Contributions: V.T.L. and S.-T.H. conceived and designed the experiments, performed the experiments, analyzed the data and wrote the paper. T.A.N.N. participated in the experimental study. H.-J.J. and H.N.H. carried out and discussed the microstructural study and reviewed the paper.

Funding: The National Research Foundation of Korea (NRF) grant (No. NRF-2015R1A5A1037627); The Encouragement Program for The Industries of Economic Cooperation Region.

Acknowledgments: This research was supported by the Ministry of Trade, Industry & Energy (MOTIE), Korea Institute for Advancement of Technology (KIAT) and Ulsan Institute for Regional Program Evaluation (IRPE) through the Encouragement Program for The Industries of Economic Cooperation Region.

Conflicts of Interest: The authors declare no conflicts of interest.

References

1. Peterson, S.F.; Mataya, M.C.; Matlock, D.K. The formability of austenitic stainless steels. *J. Miner. Met. Mater. Soc.* **1997**, *49*, 54–58. [CrossRef]
2. Andrade, M.S.; Gomes, O.A.; Vilela, J.M.C.; Serrano, A.T.L.; De Moraes, J.M.D. Formability evaluation of two austenitic stainless steels. *J. Braz. Soc. Mech. Sci. Eng.* **2004**, *26*, 47–50. [CrossRef]
3. Acar, M.O.; Fitzpatrick, M.E. Determination of plasticity following deformation and welding of austenitic stainless steel. *Mater. Sci. Eng. A* **2017**, *701*, 203–213. [CrossRef]
4. Anderson, M.; Gholipour, J.; Bridier, F.; Bocher, P.; Jahazi, M.; Savoie, J.; Wanjara, P. Improving the formability of stainless steel 321 through multistep deformation for hydroforming applications. *Trans. Can. Soc. Mech. Eng.* **2013**, *37*, 39–52. [CrossRef]
5. Thanakijkasem, P.; Uthaisangsuk, V.; Pattarangkun, A.; Mahabunphachai, S. Effect of bright annealing on stainless steel 304 formability in tube hydroforming. *Int. J. Adv. Manuf. Technol.* **2014**, *73*, 1341–1349. [CrossRef]
6. Okazaki, K.; Kagawa, M.; Conrad, H. A Study of the electroplastic effect in metals. *Scr. Metall.* **1978**, *12*, 1063–1068. [CrossRef]
7. Conrad, H. Electroplasticity in metals and ceramics. *Mater. Sci. Eng. A* **2000**, *287*, 276–287. [CrossRef]
8. Roth, J.T.; Loker, I.; Mauck, D.; Warner, M.; Golovashchenko, S.F.; Krause, A. Enhanced Formability of 5754 Aluminum Sheet Metal Using Electric Pulsing. In Proceedings of the 36th North American Manufacturing Research Conference, Monterrey, Mexico, 20–23 May 2008.
9. Salandro, W.A.; Jones, J.J.; McNeal, T.A.; Roth, J.T.; Hong, S.-T.; Smith, M.T. Formability of Al 5xxx sheet metals using pulsed current for various heat treatments. *J. Manuf. Sci. Eng.* **2010**, *132*, 1–11. [CrossRef]
10. Kim, M.-J.; Lee, K.; Oh, K.H.; Choi, I.-S.; Yu, H.-H.; Hong, S.-T.; Han, H.N. Electric current-induced annealing during uniaxial tension of aluminum alloy. *Scr. Mater.* **2014**, *75*, 58–61. [CrossRef]
11. Roh, J.-H.; Seo, J.-J.; Hong, S.-T.; Kim, M.-J.; Han, H.N.; Roth, J.T. The mechanical behavior of 5052-H32 aluminum alloys under a pulsed electric current. *Int. J. Plast.* **2014**, *58*, 84–99. [CrossRef]
12. Conrad, H. Effects of electric current on solid state phase transformations in metals. *Mater. Sci. Eng. A* **2000**, *287*, 227–237. [CrossRef]
13. Xu, Z.S.; Lai, Z.H.; Chen, Y.X. Effect of electric current on the recrystallization behavior of cold worked α–Ti. *Scr. Metall.* **1988**, *22*, 187–190. [CrossRef]

14. Park, J.-W.; Jeong, H.-J.; Jin, S.-W.; Kim, M.-J.; Lee, K.; Kim, J.J.; Hong, S.-T.; Han, H.N. Effect of electric current on recrystallization kinetics in interstitial free steel and AZ31 magnesium alloy. *Mater. Charact.* **2017**, *133*, 70–76. [CrossRef]
15. Magargee, J.; Morestin, F.; Cao, J. Characterization of flow stress for commercially pure titanium subjected to electrically assisted deformation. *J. Eng. Mater. Technol.* **2013**, *135*, 041003. [CrossRef]
16. Jeong, H.-J.; Park, J.-W.; Jeong, K.J.; Hwang, N.M.; Hong, S.-T.; Han, H.N. Effect of pulsed electric current on TRIP-aided steel. *Int. J. Precis. Eng. Manuf. Green Technol.* **2018**, in press.
17. Kim, M.-S.; Vinh, N.T.; Yu, H.-H.; Hong, S.-T.; Lee, H.-W.; Kim, M.-J.; Han, H.N.; Roth, J.T. Effect of electric current density on the mechanical property of advanced high strength steels under quasi-static tensile loads. *Int. J. Precis. Eng. Manuf.* **2014**, *15*, 1207–1213. [CrossRef]
18. Thien, N.T.; Jeong, Y.-H.; Hong, S.-T.; Kim, M.-J.; Han, H.N.; Lee, M.-G. Electrically assisted tensile behavior of complex phase ultra-high strength steel. *Int. J. Precis. Eng. Manuf. Green Technol.* **2016**, *3*, 325–333. [CrossRef]
19. Hong, S.-T.; Jeong, Y.-H.; Chowdhury, M.N.; Chun, D.-M.; Kim, M.-J.; Han, H.N. Feasibility of electrically assisted progressive forging of aluminum 6061-T6 alloy. *CIRP Ann.* **2015**, *64*, 227–280. [CrossRef]
20. Kim, M.-J.; Lee, M.-G.; Hariharan, K.; Hong, S.-T.; Choi, I.-S.; Kim, D.; Oh, K.H.; Han, H.N. Electric current-assisted deformation behavior of Al-Mg-Si alloy under uniaxial tension. *Int. J. Plast.* **2017**, *94*, 148–170. [CrossRef]
21. Williamson, G.K.; Hall, W.H. X-ray line broadening from filed aluminum and wolfram. *Acta Metall.* **1953**, *1*, 22–31. [CrossRef]
22. Ungar, T.; Borbely, A. The effect of dislocation contrast on x-ray line broadening: A new approach to line profile analysis. *Appl. Phys. Lett.* **1996**, *69*, 3173–3175. [CrossRef]
23. Cho, S.-H.; Yoo, Y.-C. Static recrystallization kinetics of 304 stainless steels. *J. Mater. Sci.* **2001**, *36*, 4273–4278. [CrossRef]